Japanese Journal of Veterinary Research 68(3): 187-195, 2020

JJVR

REGULAR PAPER Experimental Research

Cold Exposure Increases Circulating miR-122 Levels via UCP1-Dependent Mechanism in Mice

Jussiaea Valente Bariuan[1)], Yuko Okamatsu-Ogura[1,*)], Ayumi Tsubota[1)], Shinya Matsuoka[1)], Masayuki Saito[1)] and Kazuhiro Kimura[1)]

[1)] *Laboratory of Biochemistry, Faculty of Veterinary Medicine, Hokkaido University, Sapporo 060-0818, Japan*

Received for publication, February 27, 2020; accepted, May 21, 2020

Abstract

MicroRNA(miR)-122 is highly expressed in liver and secreted into blood, which is reported to enter other tissues to modulate lipid metabolism. Brown adipose tissue (BAT) is responsible for nonshivering thermogenesis required for body temperature maintenance in cold environments. Since BAT activity is deeply related to lipid metabolism, there may be metabolic crosstalk between the liver and BAT through miR-122. In this study, we examined the effect of cold exposure on circulating miR-122 (cir-miR-122) levels in mice. Cold exposure significantly increased the expressions of Uncoupling protein 1 *(Ucp1)*, a key molecule for thermogenesis, indicating the activation of BAT. Cold exposure significantly increased cir-miR-122 level but caused no change in miR-122 and its precursor levels in the liver. In contrast, cold exposure significantly decreased miR-122 level in the muscle, but not in BAT, suggesting that increased cir-miR-122 was due to the enhancement of its secretion from the muscle. To examine whether BAT thermogenesis was a prerequisite for increased cir-miR-122 and decreased miR-122 level in the muscle, effect of cold exposure was examined in UCP1-KO mice. While the expressions of thermogenesis-related genes in BAT, except for that of *Ucp1*, was increased after cold exposure, no significant changes were observed in cir-miR-122 and muscle miR-122 level in UCP1-KO mice. These results suggest that cold-induced activation of BAT thermogenesis increased cir-miR-122 through the secretion from muscle, although further study is required to find the missing link between BAT thermogenesis and miRNA secretion from the muscle.

Key Words: brown adipose tissue, cold exposure, miRNA, skeletal muscle, uncoupling protein 1

Introduction

Mammals have two types of adipose tissue [8,12)]. White adipose tissue (WAT) stores energy as triglyceride and releases fatty acids when required. Brown adipose tissue (BAT) is a specialized tissue for non-shivering thermogenesis which depends on uncoupling protein 1 (UCP1), a mitochondrial protein specifically expressed in brown adipocytes. BAT thermogenesis plays an important role in the regulation of body temperature especially in a cold environment. Cold stimulation activates sympathetic nervous system (SNS), and norepinephrine (NE) released from nerve endings activates the ß-adrenergic receptor (ß-AR), particularly ß3-AR which is predominantly expressed in adipocytes, and induces lipolysis in both white and brown adipocytes. In brown adipocytes, liberated fatty acids (FAs) activate thermogenic activity of

* Corresponding author: Yuko Okamatsu-Ogura, DVM, PhD Laboratory of Biochemistry, Faculty of Veterinary Medicine, Hokkaido University, Sapporo 060- 0818, Japan
Tel.: +81-11-706-5205 Fax: +81-11-757-0703 E-mail: y-okamatsu@vetmed.hokudai.ac.jp
doi: 10.14943/jjvr.68.3.187

UCP1 and are simultaneously used as substrates for thermogenesis [17]. FAs released from white adipocytes are also used in brown adipocytes for thermogenesis [8]. The indispensable role of BAT-UCP1 thermogenesis in the regulation of body temperature is evidenced by the fact that the mice deficient in UCP1 are unable to maintain body temperature in a cold environment [15].

MicroRNAs (miRNAs) are short, endogenous non-coding RNAs that inhibit gene expression by targeting mRNAs for translational repression or cleavage [22,26]. Several miRNA have been reported to regulate brown adipogenesis [24,28,31]. miRNAs exist not only inside of cells but also in a variety of body fluids by binding to lipids or proteins or being packed in exosome, a small extracellular vesicle stably existing in fluid [19,22]. miRNA transported to other cells, can exhibit their effects in a paracrine and endocrine-like manner [13,32]. Brown adipocytes are reported to secrete miR-92a, and the serum level of exosomal miR-92a is correlated with BAT activity in both humans and mice [10].

miR-122 is miRNA expressed abundantly in liver that are found in high levels in the circulation. As such, circulating miR-122 is used as a biomarker for variety of liver pathologic conditions [4]. Intracellular miR-122 plays a pivotal role in regulation of lipid metabolism through the direct targeting of the genes involved in triglyceride (TG) synthesis, such as *Agpat1* [21] and *Dgat1* [9], or the indirect unknown mechanism. Liver-specific knockout of miR-122 mice shows TG accumulation in liver, due to the enhancement of TG synthesis and decreased secretion [21]. On the other hand, expression and secretion of hepatic miR-122 is regulated by FAs. Chai et al., revealed that injection of ß3-AR agonist activated lipolysis in WAT, and mobilized FAs to act on liver to increase the expression and secretion of miR-122 [9]. Thus, it is likely that adipose tissue is involved in the regulation of circulating miR-122 level through FAs. Although ß3-AR agonist simultaneously induces BAT thermogenesis, the role of BAT in miR-122 metabolism has not been examined. It was also shown that the circulating miR-122 entered other tissues including muscle, and reduced triglyceride storage by targeting mRNAs of enzymes involved in the triglyceride synthesis [9].

As mentioned above, BAT uses fatty acids for thermogenesis. It is also reported that BAT activation resulted in the clearance of plasma triglyceride and cholesterol [5-7]. Since the BAT activity is deeply related with lipid metabolism, it is possible that there is metabolic organ crosstalk between the liver and BAT through miR-122. In this study we analyzed circulating miR-122 in mice with activation of BAT thermogenesis by cold exposure.

Materials and Methods

Animals

The experimental procedures and care of animals were approved by the Animal Care and Use Committee of Hokkaido University. All experiments using mice were conducted in an animal facility approved by the Association for Assessment and Accreditation of Laboratory Animal Care (AAALAC) International. UCP1-KO (*Ucp1*$^{-/-}$) mice were kindly provided by Dr. L. Kozak (Pennington Biomedical Research Center, Baton Rouge, LA, U.S.A) All wild-type (WT; *Ucp1*$^{+/+}$) mice were C57BL/6J strain. Male C57BL/6J mice were purchased from Japan SLC Inc. (Hamamatsu, Japan). Mice were bred and housed in plastic cages placed in a room temperature controlled to 23±2°C with a 12:12 hr light: dark cycle and given free access to laboratory chow (Oriental Yeast, Tokyo, Japan).

Mice of 12- to 13-week old were individually caged and placed in a room with a temperature of 10±2°C or 23±2°C for 4 hr before the sampling. We chose mild cold condition because of the cold intolerant phenotype of UCP1-KO mice [15]. The duration of cold exposure treatment was determined in the reference to the previous report where the effect of ß3-AR agonist on cir-miR-122 was examined [9]. The mice were anesthetized by intraperitoneal injection of ketamine (75 mg/

kg; Ketalar, Daiichi-Sankyo, Tokyo, Japan) and medetomidine (1 mg/kg; Domitor, Zenoaq, Fukushima, Japan) before blood sampling from the jugular vein. Ethylenediaminetetraacetic acid (EDTA) was used as an anticoagulant for the blood samples. Euthanasia via cervical dislocation was conducted and organs including the liver, interscapular BAT (iBAT), gastrocnemius muscle were quickly taken and transferred into RNAlater storage solution (Life Technologies, Carlsbad, CA, U.S.A) for miRNA analysis.

Blood samples were centrifuged at 2000 rpm for 30 min to harvest the plasma. Samples that were still cloudy after 30 min of centrifuge were centrifuged at 3000 rpm for an additional 30 min before storage. Samples were stored at -80°C until use.

Extraction of miRNA and total RNA

Extraction of miRNA from plasma and tissue was achieved using miRNeasy kit (QIAGEN, Hilden Germany). For plasma samples, 100 µL of QIAzol reagent (QIAGEN) was added to 20 µL of isolated plasma and incubated for 5 min at room temperature. After the addition of 10 µL of 1 nM Cel-miR-39-3p spike-in (QIAGEN) and 20 µL of chloroform, samples were centrifuged at 12,000 x g for 15 min at 4 °C. For tissue samples, 10-20 mg of tissues stored in RNAlater were placed in a tube and 1 mL of QIAzol reagent was added. The samples were then homogenized using Mixer Mill 300 (Retsch, Haan, Germany), for 1 min and centrifuged after at 12,000 x g for 15 min at 4 °C. The upper aqueous phase of each sample, both plasma and tissue, was carefully transferred to a fresh tube, and 1.5 volumes of ethanol was added. Each sample was then applied directly to columns and after washing, miRNA was eluted in 12 and 40 µl of nuclease-free water for plasma and tissue samples, respectively. The quantity of miRNA was measured with Qubit microRNA assay kit (Thermo Fisher Scientific, Eugene, OR, U.S.A) reagents using a Qubit 3.0 Fluorometer (Thermo Fisher Scientific). Extraction of total RNA from tissue was achieved using TRIzol (Thermo Fisher Scientific) according to the manufacturer's instructions.

Real-time PCR

The extracted miRNA was reverse transcribed using a miR-X miRNA First Strand Synthesis kit (Clontech, Palo Alto, CA, U.S.A). Briefly, 1.5 µl of miRNA, with concentrations ranging from 0.4 to 0.6 ng/µL, was mixed with an mRQ enzyme and incubated at 37 °C for 1 h and then at 85 °C for 5 min. After the addition of 100 µl of ultrapure water, 2 µl of the sample was used for real-time PCR. For mRNA analysis, total RNA (2 µg) was reverse-transcribed using a 15-mer oligo(dT) adaptor primer and M-MLV reverse transcriptase (Promega, Madison, WI, U.S.A).

Real-time PCR was performed on a fluorescence thermal cycler (Light Cycler system, Roche Diagnostics, Mannheim, Germany) with FastStart Essential DNA Green Master (Roche Diagnostics), and primers specific to each miRNA or mRNA. For miRNA analysis, mRQ3' primer supplied by miRX miRNA First Strand Synthesis kit (Clontech) and miRNA-specific primer prepared according to the kit manual were used. Other primers used in the study are listed in Table 1.

Expressions of miRNA were normalized to Cel-miR-39-3p or small nuclear RNA U6 *(snRU6)* as reference. Expressions of mRNA were normalized to the expression levels of *Actb*.

Plasma non-esterified fatty acid (NEFA) and exosomal CD63 measurement

Plasma NEFA concentration was assayed using a NEFA C kit (Wako, Osaka, Japan) following the manufacturer's instructions.

Exosome level was measured using PS Capture Exosome ELISA Kit Anti Mouse IgG POD (Wako) according to the manufacturer's instructions with a slight modification. Briefly, plasma samples were incubated with stirring at room temperature for 2 hr in the Exosome Capture 96 Well Plate. After washing, anti-mouse CD63 monoclonal antibody (Biolegend,

Table 1. Primer sequences for quantitative real-time PCR.

Gene name (gene symbol): NCBI Reference Sequence number, Product size Forward, and reverse primer sequence
Small nuclear U6 (snRU6): XR_003953346.1, 107 bp
5' – CTCGCTTCGGCAGCACA - 3', 5' – AACGCTTCACGAATTTGCGT – 3'
Actin beta (Actb): NM_007393.5, 234 bp
5' – TCG TTA CCA CAG GCA TTG TGA T - 3', 5' – TGC TCG AAG TCT AGA GCA AC – 3'
Uncoupling protein 1 (Ucp1): NM_009463.3, 197 bp
5' – GTG AAG GTC AGA ATG CAA GC - 3', 5' – AGG GCC CCC TTC ATG AGG TC – 3'
Iodothyronine deiodinase 2 (Dio2): NM_010050.4, 130bp
5' – CAG TGT GGT GCA CGT CTC CAA TC – 3', 5' – TGA ACC AAA GTT GAC CAC CAG – 3'
Fibroblast growth factor 21 (Fgf21): NM_020013.4, 154bp
5' – CTG CTG GGG GTC TAC CAA G – 3', 5' – CTG CGC CTA CCA CTG TTC C – 3'
PR domain containing 16 (Prdm16): XM_006539175.4, 180bp
5' – GAC ATT CCA ATC CCA CCA GA – 3', 5' – CAC CTC TGT ATC CGT CAG CA – 3'
Cell death-inducing DNA fragmentation factor alpha (Cidea): NM_007702.2, 222bp
5' – CTT ATC AGC AAG ACT CTG GAT G – 3', 5' – GAA GGT GAC TCT GGC TAT TC – 3'
Cytochrome c oxidase subunit 4 (Cox4): NM_009941.3, 252 bp
5' – TGA GCC TGA TTG GCA AGA GA – 3', 5' – CGA AGC TCT CGT TAA ACT GG – 3'
Epithelial V-like antigen 1 (Eva1): NM_007962.4, 111bp
5' – CCA CTT CTC CTG AGT TTA CAG C – 3', 5' – GCA TTT TAA CCG AAC ATC TGT CC – 3'

CA, U.S.A) was added and incubated at room temperature for 1 hr. The plate was washed again and HRP-conjugated anti-mouse IgG was added and allowed to incubate with shaking at room temperature for 1 hr. The plate was washed again before reacting with TMB Solution at room temperature for 30 min. Stop Solution was added and absorbance was measured at 450 nm.

Data analysis

Statistical analyses were performed using the SPSS Statistics Version 23 software package from IBM (Chicago, IL, U.S.A). Differences between the treatment groups were analyzed by Student's t-test. P-values < 0.05 were considered to be statistically significant.

Results

First, we exposed mice to a cold temperature of 10°C for 4 hr and examined the gene expression in BAT. Cold exposure significantly increased the expression of the BAT marker, *Ucp1*, by 2-fold (Fig.1), indicating the activation of BAT. As reported previously [14], the expressions of *Dio2* and *Fgf21* were also significantly increased by cold exposure. The change in the expressions of other genes related to BAT thermogenic function including *Prdm16*, *Cidea*, and *Eva1* was negligible in this condition.

Next, we examined the effect of cold exposure on cir-miR-122. Cir-miR-122 levels of cold exposed mice increased by 3-fold compared to the control mice kept at 23°C (Fig 2A). However, cold exposure did not alter the plasma NEFA concentration (Fig 2B) and exosome level (Fig 2C). These results indicate that cold exposure increased cir-miR-122 was not due to plasma fatty acid level changes.

To identify the source of cir-miR-122 in cold-exposed mice, hepatic content of miR-122 was measured. Cold exposure did not show any changes in both hepatic miR-122 (Fig 3A) and

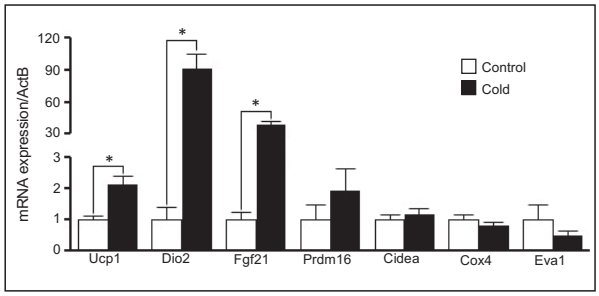

Fig. 1. Effect of cold exposure on thermogenic gene expressions in BAT of wild-type mice.

Wild-type mice were exposed to 23°C (Control) or 10°C (Cold) for 4 hr. Expressions of thermogenic genes in BAT were measured by real-time PCR. Data were normalized to *ActB* expression and expressed relative to the value of control group. Values are expressed as means ± SE (n=11 for control and n=8 for cold group). **P* < 0.05, Student's t-test.

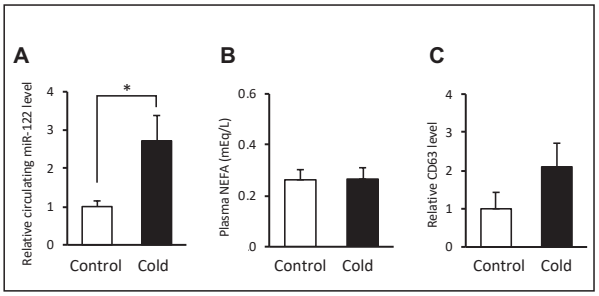

Fig. 2. miR-122 levels, NEFA concentration, and CD63 levels in the circulation of wild-type mice after cold exposure.

Mice were exposed to 23°C (Control) or 10°C (Cold) for 4 hr. Blood was taken from the jugular vein, and plasma miR122 levels (A), NEFA concentrations (B), and CD63 levels (C) were measured. Circulating miR-122 levels were measured by real-time PCR and normalized to the levels of spike-in cel-miR-39a. Values are expressed as means ± SE (n=11 for control and n=8 for cold group). Values are expressed as means ± SE. **P* < 0.05, Student's t-test.

pre-miR-122 levels (Fig 3B), suggesting that the increase in cir-miR-122 induced by cold exposure was unlikely due to the production nor the secretion from the liver. To examine the involvement of other tissues, iBAT and skeletal muscle were analyzed. The miR-122 level was not affected in iBAT (Fig 3C), but significantly decreased in muscle (Fig 3D).

UCP1-KO mice were used to directly examine the relation between the cold-induced BAT thermogenesis and the change in cir-miR-122 levels. Cold exposure for 4 hr in UCP1-KO mice caused significant increase in the expression of *Dio2* and *Cidea*, and not in *Fgf21*, *Prdm16*, and *Eva1*, although there was a tendency of increase (Fig.4A). These results indicate the cold exposure was sufficient in inducing the SNS-NE-ß-AR pathway for BAT thermogenesis in UCP1-KO mice [14]. In contrast to the response of WT mice, cold exposure did not change cir-miR-122 level, as well as plasma NEFA concentration and exosome level, in UCP1-KO mice (Fig 4B-D). Hepatic miR-122 level also failed to show any change in cold-exposed UCP1-KO mice (Fig 4E). MiR-122 level in BAT and skeletal muscle also did not change after cold exposure in UCP1-KO mice (Fig 4 F-G).

Discussion

In this study, we examined the effect of cold exposure on the cir-miR-122 levels in mice. Previously, it was reported that the injection of ß3-AR agonist CL316,243 increased expression and secretion of hepatic miR-122 and therefore cir-miR-122, through its action on WAT to mobilize FAs in circulation [9]. In addition to WAT lipolysis, ß3-AR agonist also induces BAT thermogenesis, however, the role of BAT in miR-122 metabolism has not been examined. Cold exposure is a potent physiological stimuli to induce BAT thermogenesis: it activates SNS, which leads to the stimulation of ß3-AR in BAT and WAT, as well as other types of adrenoceptor in many tissues. We found that cold exposure at 10°C for 4 hr resulted in a modest increase in cir-miR-122, without alteration of the plasma NEFA concentration. Thus, the increases in cir-miR-122 after cold exposure is likely independent of the effect of FAs on liver. In agreement with this idea, hepatic miR-122 level showed no change upon cold exposure. Although liver is known as a major source of cir-miR-122, it is plausible that the cold-induced elevation of cir-miR-122 may be not through the secretion from liver.

Since the cold exposure induces shivering and

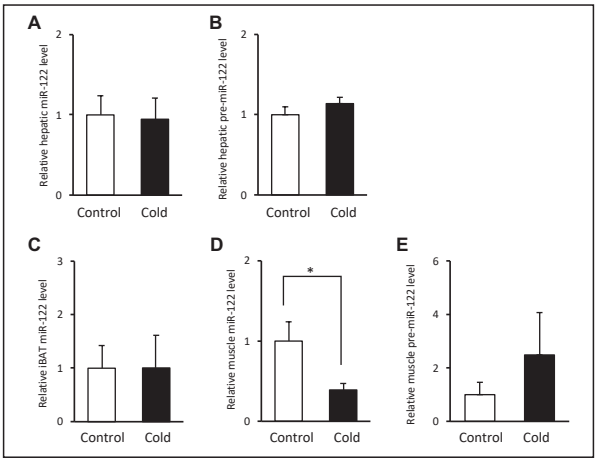

Fig. 3. Content of miR-122 and pre-miR-122 in tissues of wild-type mice after cold exposure.

Mice were exposed to 23°C (Control) or 10°C (Cold) for 4 hr. Tissue samples were taken and miR-122 levels in liver (A), gastrocnemius muscle (C) and BAT (D) (n=11 for control and n=8 for cold group) and pre-miR-122 in liver (B) (n=4 for control and cold groups) were measured by real-time PCR. Data were normalized to the levels of small nuclear RNA U6. Values are expressed as means ± SE. *$P < 0.05$, Student's t-test.

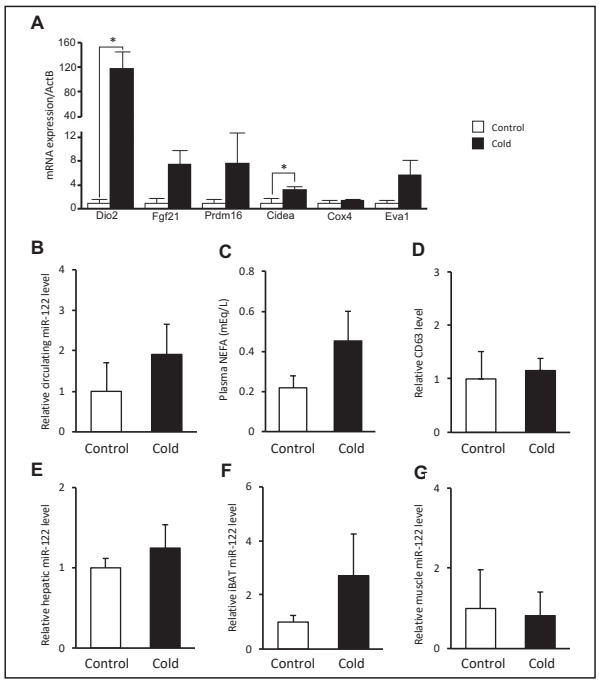

Fig. 4. Effect of cold exposure on gene expressions, plasma parameters, and tissue miR-122 levels in UCP1-KO mice.

UCP1-KO mice were exposed to 23°C (Control) or 10°C (Cold) for 4 hr. Expressions of thermogenic genes in BAT were measured by real-time PCR (A). Plasma miR-122 levels (B), NEFA concentrations (C) (n=6 for control and n=4 for cold group), and CD63 levels (D) (n=4 for control and cold groups) were measured. The miR-122 levels in liver (E), BAT (F), and gastrocnemius muscle (G) were also measured (n=6 for control and n=4 for cold group). Values are expressed as means ± SE. *$P < 0.05$, Student's t-test.

non-shivering thermogenesis [2,3,8], we examined the involvement of their responsible tissues, BAT and skeletal muscle, as a source of miR-122 upon cold exposure. miR-122 levels in BAT did not show any significant change after the cold exposure, whereas those in muscle were significantly decreased in the cold-exposed mice compared to the control mice. These results suggest that the release of miR-122 from muscle may contribute to the increase in cir-miR-122. It has been reported that skeletal muscle release various kinds of exosomal miRNAs that function in a paracrine or endocrine manner. For example, exosomal miRNAs derived from myotube were reported to downregulate Sirtuin1 (Sirt1) expression in myoblasts and affect their differentiation [18]. In addition, muscle-derived microRNAs that affect skeletal muscle development [20] or those increased after acute exercise [19] were reported. Thus, it is possible that muscle secretes miRNAs upon cold exposure. Since we found that miR-122 level in muscle is very low compared to that in liver (> 200-fold lower in muscle than that in liver), the physiological significance of this pathway is unknown. However, since skeletal muscle is the largest organ as total mass in whole body than other organs, it may give a significant contribution to circulating level of miR-122. Otherwise, it is also likely that muscle releases miR-122 to the circulation to reduce its intracellular level. In liver, the inhibition of miR-122 is reported to enhance fatty acid oxidation [16], possibly through the increase in the expression of target gene Sirt1 and subsequent activation of AMP-activated protein kinase pathway [25]. Thus, the reduced intracellular level of miR-122 in muscle may result in the increase in fatty acid oxidation, contributing to the effective supply of energy source for shivering thermogenesis.

In contrast to the results in WT mice, cold exposure in UCP1-KO mice did not cause the increase in the cir-miR-122 nor decrease in miR-122 in muscle, indicating that activation of UCP1 thermogenesis in BAT is essential for the release of miR-122 from muscle. It is not clear how the

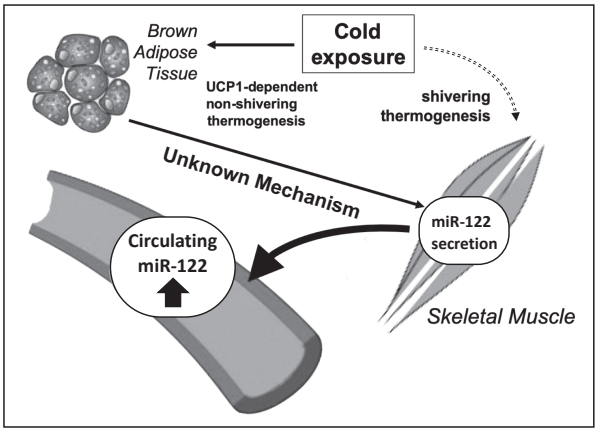

Fig. 5. Scheme of suggested mechanism for cold exposure-induced increase in circulating miR-122.
Cold exposure stimulates UCP1-dependent thermogenesis in BAT. BAT thermogenesis leads to the secretion of miR-122 from skeletal muscle through an unknown mechanism, resulting in the increase in circulating miR-122 (cir-miR-122). Shivering thermogenesis in skeletal muscle is also induced by cold exposure, but results from UCP1-KO mice suggest that it is irrelevant to the cir-miR-122 increase.

status of UCP1 activity in BAT was transmitted to muscle. Recently, it was reported that cold stimulation induces the release of succinate from muscle, and it is subsequently taken up by BAT, activating UCP1 thermogenesis [27]. Although it is unknown if the release of succinate is dependent on BAT activity, it is plausible that there is some inter-organ communication between BAT and muscle. It is also possible that the miR-122 release from muscle did not occur in UCP1-KO mice because of a compensatory phenotypic change for the loss of UCP1. It has been reported that non-shivering thermogenesis in muscle depending on SERCA or sarcolipin compensates the loss of UCP1-dependent thermogenesis in the BAT of UCP1-KO mice [2,3,29,30]. Such compensatory changes of muscle may possibly associate with the lack of the miR-122 release from muscle in UCP1-KO mice.

In summary, we found that cir-miR-122 is increased after cold exposure possibly through the secretion from muscle (Fig. 5). In addition, we found that the cold-induced increase in cir-miR-122 was dependent on UCP1-thermogenesis in BAT. It is not clear how BAT thermogenesis induced miR-122 secretion from muscle, however, there may be some cross talk between BAT and muscle as that reported between BAT and liver [1,11,33]. Further study is required to reveal the precise mechanism for the cold-induced increase in the cir-miR-122.

Acknowledgements

This study was supported by JSPS KAKENHI Grant Numbers 16K15485, 17K08118, 18H02274, and 18J21697.

References

1) Ameka M, Markan KR, Morgan DA, BonDurant LD, Idiga SO, Naber MC, Zhu Z, Zingman LV, Grobe JL, Rahmouni K, Potthoff MJ. Liver derived FGF21 maintains core body temperature during acute cold exposure. Sci Rep 9, 630, 2019.
2) Bal NC, Maurya SK, Sopariwala DH, Sahoo SK, Gupta SC, Shaikh SA, Pant M, Rowland LA, Bombardier E, Goonasekera SA, Tupling AR, Molkentin JD, Periasamy M. Sarcolipin is a newly identified regulator of muscle-based thermogenesis in mammals. Nat Med 18, 1575-1579, 2012.
3) Bal NC, Singh S, Reis FCG, Maurya SK, Pani S, Rowland LA, Periasamy M. Both brown adipose tissue and skeletal muscle thermogenesis processes are activated during mild to severe cold adaptation in mice. J Biol Chem 292, 16616-16625, 2017.
4) Bandiera S, Pfeffer S, Baumert TF, Zeisel MB. miR-122--a key factor and therapeutic target in liver disease. J Hepatol 62, 448-457, 2015.
5) Bartelt A, Bruns OT, Reimer R, Hohenberg H, Ittrich H, Peldschus K, Kaul MG, Tromsdorf UI, Weller H, Waurisch C, Eychmüller A, Gordts PL, Rinninger F, Bruegelmann K, Freund B, Nielsen P, Merkel M, Heeren J. Brown adipose tissue activity controls triglyceride clearance. Nat Med 17, 200-205, 2011.

6) Bartelt A, John L, Schaltenberg N, Berbée JFP, Worthmann A, Cherradi ML, Schlein C, Piepenburg J, Boon MR, Rinninger F, Heine M, Toedter K, Andreas N, Stefan KN, Markus F, Wijers SL, Lichtenbelt WM, Scheja L, Rensen PCN, Heeren J. Thermogenic adipocytes promote HDL turnover and reverse cholesterol transport. Nat Commun 8, 15010, 2017.
7) Berbée JFP, Boon MR, Khedoe PP, Bartelt A, Schlein C, Worthmann A, Kooijman S, Hoeke G, Mol IM, John C, Jung C, Vazirpanah N, Brouwers LP, Gordts PL, Esko JD, Hiemstra PS, Havekes LM, Scheja L, Heeren J, Rensen PC. Brown fat activation reduces hypercholesterolaemia and protects from atherosclerosis development. Nat Commun 6, 6356, 2015.
8) Cannon B and Nedergaard J. Brown adipose tissue: function and physiological significance. Physiol Rev 84, 277-359, 2004.
9) Chai C, Rivkin M, Berkovits L, Simerzin A, Zorde-Khvalevsky E, Rosenberg N, Klein S, Yaish D, Durst R, Shpitzen S, Udi S, Tam J, Heeren J, Worthma A, Galun E. Metabolic circuit involving free fatty acids, microRNA 122, and triglyceride synthesis in Liver and muscle tissues. Gastroenterology 153, 1404-1415, 2017.
10) Chen Y, Buyel JJ, Hanssen MJW, Siegel F, Pan R, Naumann J, Schell M, van derLans A, Schlein C, Froehlich H, Heeren J, Virtanen KA, Lichtenbelt WM, Pfeifer A. Exosomal microRNA miR-92a concentration in serum reflects human brown fat activity. Nat Comm 7, 11420, 2016.
11) Chen Z, Wang GX, Ma SL, Jung DY, Ha H, Altamimi T, Zhao XY, Guo L, Zhang P, Hu CR, Cheng JX, Lopaschuk GD, Kim JK, Lin JD. Nrg4 promotes fuel oxidation and a healthy adipokine profile to ameliorate diet-induced metabolic disorders. Mol Metab 6, 863-872, 2017.
12) Cinti S. The adipose organ at a glance. Dis Model Mech 5, 588-594, 2012.
13) Cortez MA, Bueso-Ramos C, Ferdin J, Lopez-Berestein G, Sood AK, Calin GA. MicroRNAs in body fluids—the mix of hormones and biomarkers. Nat Rev Clin Oncol 8, 467-477, 2011.
14) DeJong JM, Larsson O, Cannon B, Nedergaard J. A stringent validation of mouse adipose tissue identity markers. Am J Physiol. Endocrinol Metab 308, E1085-E105, 2015.
15) Enerback S, Jacobsson A, Simpson EM, Guerra C, Yamashita H, Harper ME, Kozak LP. Mice lacking mitochondrial uncoupling protein are cold-sensitive but not obese. Nature 387, 90-94, 1997.
16) Esau C, Davis S, Murray SF, Yu XX, Pandey SK, Pear M, Watts L, Booten SL, Graham M, McKay R, Subramaniam A, Propp S, Lollo BA, Freier S, Bennett CF, Bhanot S, Monia BP. miR-122 regulation of lipid metabolism revealed by in vivo antisense targeting. Cell Metab 3, 87-98, 2006.
17) Fedorenko A, Lishko PV, Kiszrichok Y. Mechanism of fatty-acid-dependent UCP1 uncoupling in brown fat mitochondria. Cell 151, 400-413, 2012.
18) Forterre A, Jalabert A, Chikh K, Pesenti S, Euthine V, Granjon A, Errazuriz E, Lefai E, Vidal H, Rome S. Myotube-derived exosomal miRNAs downregulate Sirtuin1 in myoblasts during muscle cell differentiation. Cell Cycle 13, 78-89, 2014.
19) Guescini M, Canonico B, Lucertini F, Maggio S, Annibalini G, Barbieri E, Luchetti F, Papa S, Stocchi V. Muscle releases alpha-sarcoglycan positive extracellular vesicles carrying miRNAs in the bloodstream. PloS One 10, e0125094-e0125094, 2015.
20) Horak M, Novak J, Bienertova-Vasku J. Muscle-specific microRNAs in skeletal muscle development. Dev Biol 410, 1-13, 2016.
21) Hsu SH, Wang B, Kota J, Yu J, Costinean S, Kutay H, Yu L, Bai S, La Perle K, Chivukula RR, Mao H, Wei M, Clark KR, Mendell JR, Caligiuri MA, Jacob ST, Mendell JT, Ghoshal

K. Essential metabolic, anti-inflammatory, and anti-tumorigenic functions of miR-122 in liver. J Clin Invest 122(8), 2871-83, 2012.
22) Huang-Doran I, Zhang CY, Vidal-Puig A. Extracellular vesicles: novel mediators of cell communication in metabolic disease. Trends Endocrinol Metab 28, 3-18, 2017.
23) Krol J, Loedige I, Filipowicz W. The widespread regulation of microRNA biogenesis, function and decay. Nat Rev Genet 11, 597-610, 2010.
24) Liu W, Bi P, Shan T, Yang X, Yin H, Wang YX, Liu N, Rudnicki MA, Kuang S. miR-133a regulates adipocyte browning in vivo. PLoS Genet 9, e1003626, 2013.
25) Long JK, Dai W, Zheng YW, Zhao SP. miR-122 promotes hepatic lipogenesis via inhibiting the LKB1/AMPK pathway by targeting Sirt1 in non-alcoholic fatty liver disease. Mol Med 25(1), 2, 2019.
26) Lorente-Cebrián S, González-Muniesa P, Milagro FI, Martínez JA. MicroRNAs and other non-coding RNAs in adipose tissue and obesity: emerging roles as biomarkers and therapeutic targets. Clin Sci 133, 23-40, 2019.
27) Mills EL, Pierce KA, Jedrychowski MP, Garrity R, Winther S, Vidoni S, Yoneshiro T, Spinelli JB, Lu GZ, Kazak L, Banks AS, Haigis MC, Kajimura S, Murphy MP, Gygi SP, Clish CB, Chouchani ET. Accumulation of succinate controls activation of adipose tissue thermogenesis. Nature 560, 102-106, 2018.
28) Mori M, Nakagami H, Rodriguez-Araujo G, Nimura K, Kaneda Y. Essential role for miR-196a in brown adipogenesis of white fat progenitor cells. PLoS Biol 10, e1001314, 2012.
29) Nowack J, Giroud S, Arnold W, Ruf T. Muscle non-shivering thermogenesis and its role in the evolution of endothermy. Front Physiol 8, 889, 2017.
30) Shabalina IG, Hoeks J, Kramarova TV, Schrauwen P, Cannon B, Nedergaard J. Cold tolerance of UCP1-ablated mice: A skeletal muscle mitochondria switch toward lipid oxidation with marked UCP3 up-regulation not associated with increased basal, fatty acid- or ROS-induced uncoupling or enhanced GDP effects. Biochim Biophys, Acta, Bioenerg 1797, 968–980, 2010.
31) Shamsi F, Zhang H, Tseng YH. MicroRNA regulation of brown adipogenesis and thermogenic energy expenditure. Front Endocrinol 8, 205, 2017.
32) Thomou T, Mori MA, Dreyfuss JM, Konishi M, Sakaguchi M, Wolfrum C, Rao TN, Winnay JN, Garcia-Martin R, Grinspoon SK, Gorden P, Kahn CR. Adipose-derived circulating miRNAs regulate gene expression in other tissues. Nature 542, 450-455, 2017.
33) Villarroya F, Gavaldà-Navarro A, Peyrou M, Villarroya J, Giralt M. The lives and times of brown adipokines. Trends in Endocrin Met 28, 855–867, 2017.